This is an open access article published under an ACS AuthorChoice License, which permits copying and redistribution of the article or any adaptations for non-commercial purposes.

THE JOURNAL OF PHYSICAL CHEMISTRY Letters

Letter

pubs.acs.org/JPCL

Synergistic Effects in the Coupling of Plasmon Resonance of Metal Nanoparticles with Excited Gold Clusters

Kevin G. Stamplecoskie and Prashant V. Kamat*

Notre Dame Radiation Laboratory, Department of Chemistry and Biochemistry, University of Notre Dame, Notre Dame, Indiana 46556, United States

Supporting Information

ABSTRACT: When molecules or clusters are within the proximity of metal particles, their electronic transitions can be drastically enhanced. We have now probed the off-resonance excitation of molecule-like, glutathione-capped gold clusters (Au-GSH) in the close proximity of larger (plasmonic) Au and Ag nanoparticles. The excited state absorption spectrum of Au-GSH* is obtained with monophotonic excitation. The characteristic absorption of Au-GSH* allows us to probe the influence of excited plasmonic nanoparticles coupled with the clusters. Although infrared (775 nm) lasers pulses do not produce Au-GSH*, the excited states of these clusters are formed when coupled with metal (Au, Ag) nanoparticles. Interestingly, the coupled excitation of Au-GSH/AgNP with 775 nm laser pulses also results in an enhanced field effect, as seen from increased plasmon response of the metal nanoparticles. Transient absorption measurements confirm the synergy between these two inherently different nanomaterials, causing them to display greater excitation features. Better understanding of metal cluster−metal nanoparticle interactions will have important implications in designing light harvesting systems, and optoelectronic devices.

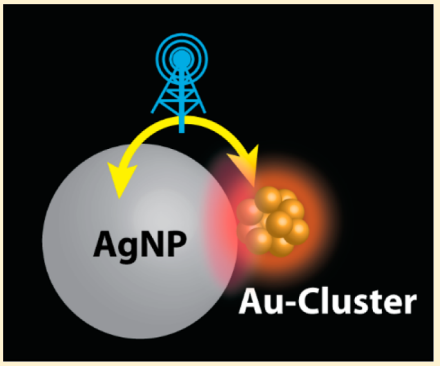

Metal nanoparticles occupy an important sector of nanomaterials research, largely due to their unique optical properties as compared to their bulk metal counterparts.[1] Most notably, plasmon excitation of colloids like silver (AgNP) and gold (AuNP) can be achieved with visible light.[2−5] Plasmon excitation causes a coherent oscillation of electrons in the nanoparticles, which generates a strong electromagnetic field.[1,4] The electromagnetic field has been used to enhance optical transitions in neighboring molecules and semiconductors, enhance the quantum yield of photochemical reactions, and is commonly employed in surface enhanced Raman spectroscopy and infrared absorption spectroscopy.[4,6−10]

When the size of metal nanoparticles becomes very small (<1 nm), with a precise number of metal atoms and capped with a stabilizing ligand, they are referred to as "clusters". In contrast to nanoparticles, the band structure for clusters breaks down into discrete, molecule-like, electronic states.[11−16] Hence, they do not support localized surface plasmon absorptions, and their absorption properties are dictated by electronic transitions similar to molecules. The optical transitions of these clusters are strongly dependent on the exact number of metal atoms in the clusters.[17−21] Unlike nanoparticles, these clusters have long-lived excited states (hundreds of nanoseconds) and relatively high quantum yields of emission.[22,23]

Metal nanoparticles have been used in many light-harvesting applications, mainly for their plasmon enhancement effects.[24−26] When these nanoparticles are made, however, there is often a large polydispersity in size. When a polydispersity exists, the origin of optical activity is a subject of debate, whether the activity arises from the presence of small, molecule-like, metal clusters or plasmon enhancement effects of nanoparticles. Moreover, the optical/electronic interaction between clusters and nanoparticles can also affect the overall photoactivity of the metal nanostructures. The main goal of this work is to elucidate the interaction between these optically different metal clusters/nanoparticles. Au-GSH clusters have been shown to exhibit red emission with a 2.0% quantum yield and an excited state lifetime of ∼780 ns.[22,27] In order to assess the metal cluster−metal NP interactions, we have now probed the excited state properties of glutathione-protected gold clusters (Au-GSH) coupled to AgNPs. Transient absorption spectroscopy is used to elucidate the synergy arising from optical interactions (i.e., plasmon enhancement) between the two materials.

AgNPs deposit uniformly on Al_2O_3 and have a relatively large size distribution, as seen from Figure 1B, whereas Au-GSHs form a more dense distribution over the surface of Al_2O_3. The Au-GSH clusters used here have a narrow size distribution because they vary in gold atom number, with 29−43 metal atoms per cluster.[28] These Au-GSH clusters uniformly cover the Al_2O_3 substrate, as seen from Figure 1C,D.

The absorption spectra of AgNP, Au-GSH clusters, and coupled AgNP−AuGSH clusters, following deposition onto Al_2O_3 films, are shown in Figure 1E (spectra b, c, and d, respectively). AgNPs deposited on Al_2O_3 exhibit characteristic

Received: March 31, 2015
Accepted: April 30, 2015
Published: April 30, 2015

 © 2015 American Chemical Society

DOI: 10.1021/acs.jpclett.5b00665
J. Phys. Chem. Lett. 2015, 6, 1870−1875

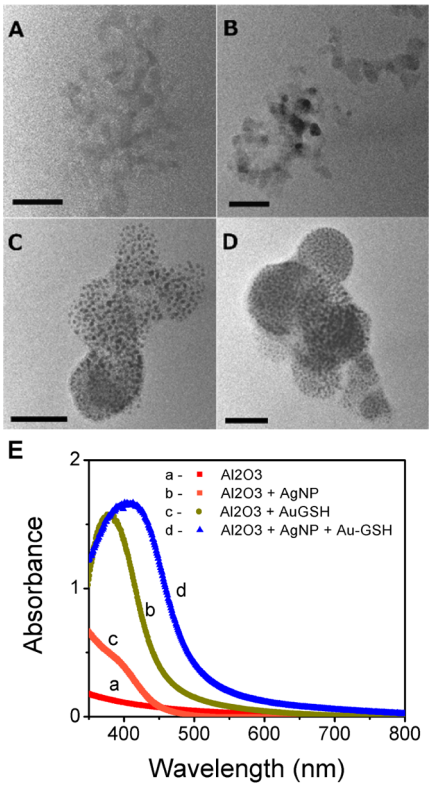

Figure 1. TEM images of Al_2O_3 substrate (A), Al_2O_3 with deposited AgNP (B), Al_2O_3 with adsorbed Au-GSH (C), and Al_2O_3 with both AgNP and Au-GSH (D), and the absorbance spectra of each of the films in A–D shown in (E). Scale bars in A–D are all 50 nm.

plasmon absorption at 400 nm. Au-GSH clusters exhibit featureless absorption, with a shoulder at 420 nm. The coupled AgNP-AuGSH show a broad absorption, which is essentially an additive spectral feature of b and c. We have probed the interaction of AgNP with AuGSH using both 387 and 775 nm laser excitations. Au-GSH can be directly excited with a 387 nm pulsed laser as evidenced by its excited state with a broad characteristic transient absorption spectrum.[22] However, these clusters cannot be directly excited with 775 nm laser pulses. AgNP, on the other hand, can be excited through both (a) linear absorption of 387 nm laser pulses, as well as (b) two-photon excitation using 775 nm laser pulses.[29] We also conducted similar measurements using AuNP. The interaction of Au-GSH clusters with AuNP exhibits results similar to those carried out with AgNP. These results with AuNP are presented separately in the Supporting Information (Figures S2–4) for simplicity and clarity of discussion. It should be noted that AgNP is a better example to investigate the metal NP–AuGSH interactions since the plasmon absorption maximum for AgNP can be separated from the Au-GSH* signal, making it easier to resolve spectral features in the transient spectrum.

Monophotonic Excitation with 387 nm Laser Pulses. AgNP, when excited with a 387 nm laser pulse, exhibits dampening of the plasmon peak resulting in bleaching at wavelengths less than 450 nm and an induced absorption at 470 nm in the transient absorption spectrum (Figure 2A). The rest of the visible region (>550 nm), following AgNP excitation, exhibit negligible changes in the absorption. Also shown in Figure 2B,C (spectra d and f) are transient absorption spectra of Au-GSH and AgNP-coupled Au-GSH clusters on Al_2O_3 films recorded 1 ps after 387 nm laser pulse excitation (reaction 1).

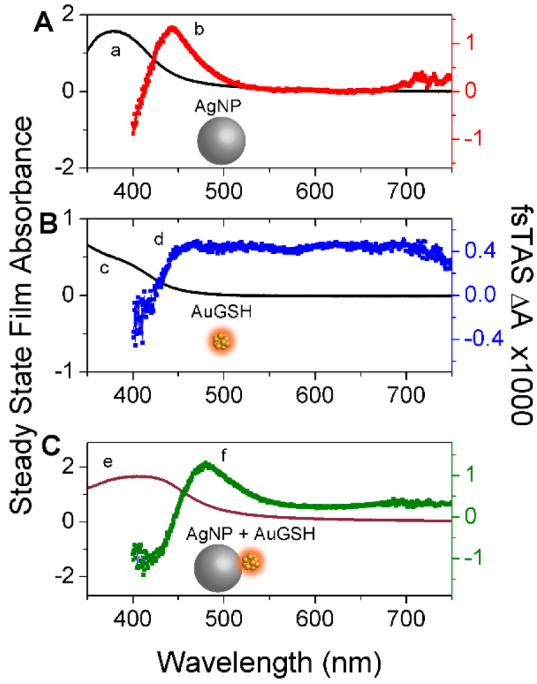

Figure 2. Steady state absorbance (a,c,e) and difference absorbance (transient) spectra (b,d,f) of Al_2O_3 films containing (A) AgNP, (B) AuGSH alone, and (C) and AgNP/AuGSH. The transient spectra were recorded 1 ps after 387 nm laser pulse excitation.

$$\text{Au-GSH} + h\nu_{387\text{nm}} \rightarrow \text{Au-GSH}^* \quad (1)$$

$$\text{AgNP} + h\nu_{387\text{nm}} \rightarrow \text{AgNP}^* \quad (2)$$

$$\text{Au-GSH/AgNP} + h\nu_{387\text{nm}} \rightarrow \text{Au-GSH}^*/\text{AgNP}^* \quad (3)$$

AuGSH* clusters show a broad absorption in the visible, while AgNP-coupled AuGSHs show an additional bleaching in the 400 nm region. It is evident that trace f exhibits an additive effect of A and B, as 387 nm results in excitation of both AgNP and AuGSH.

The decay of the excited state following laser excitation is monitored at 650 nm for each of AgNP, Au-GSH, and AgNP/Au-GSH (Figure 3). Excited AgNPs show a quick decay (~2 ps) of the transient absorption as the hot electrons are relaxed within the particle (trace a). AuGSH* exhibits no noticeable decay during the initial 10 ps period (trace b in Figure 3). The

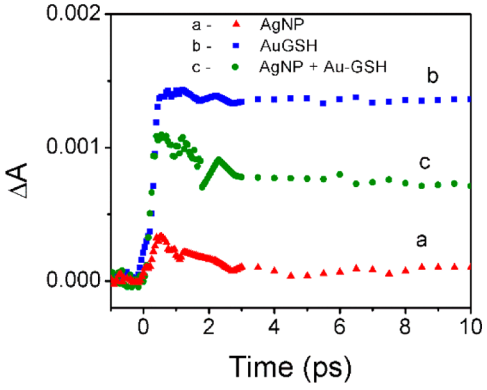

Figure 3. Kinetic traces for the decay of the transient absorption after 387 nm femtosecond pulsed excitation of AgNP (a), AuGSH (b) and AgNP coupled to AuGSH (c), monitored at 650 nm.

DOI: 10.1021/acs.jpclett.5b00665
J. Phys. Chem. Lett. 2015, 6, 1870–1875

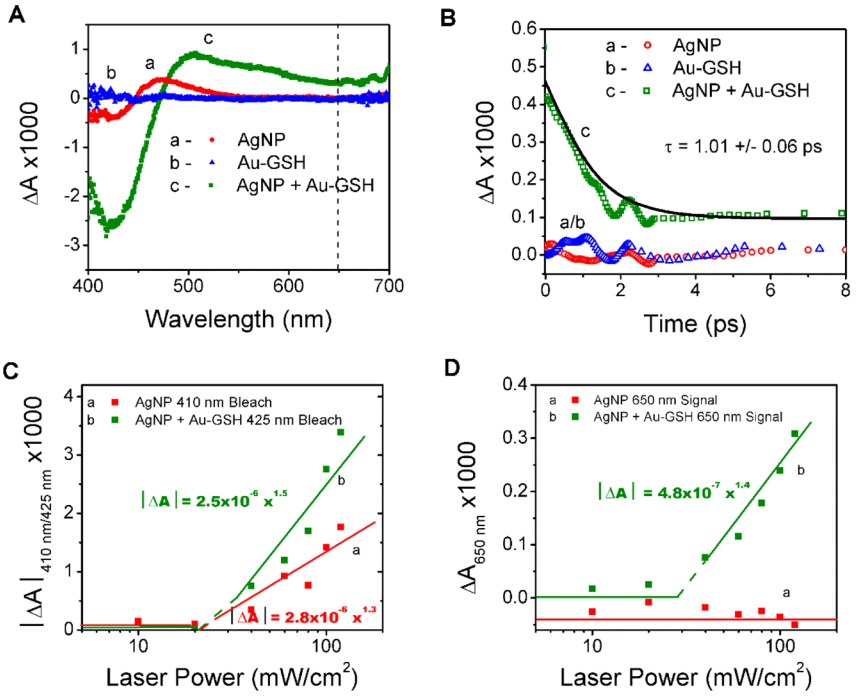

Figure 4. (A) Difference absorbance spectra of Al_2O_3 films containing (a) AgNP alone, (b) AuGSH alone, and (c) AgNP/Au-GSH, recorded 1 ps after 775 nm laser pulse excitation and, (B) transient absorption decay profile for each sample in a/b/c monitored at 650 nm. The dashed line in panel A indicates the wavelength monitored in panel B, where it is possible to observe the excited state absorption of Au-GSH* without overlap with the AgNP plasmon absorption. The line in B is the fitting of the excited state decay to a monoexponential decay that yields a lifetime of 1.01 ± 0.06 ps. The change in absorption of 1 ps after 775 nm laser pulse excitation as a function of power, monitored at the plasmon bleach maximum (410 nm for AgNP and 425 nm for AgNP/Au-GSH) in panel C, and at 650 nm in panel D. The values of η, determined from the slope of the linear plots in C and D are 1.5/1.3 and 1.4 for the AgNP and Au-GSH signals, respectively (see Expression 7).

decay of the 650 nm transient absorption corresponding to AgNP/Au-GSH excitation is mostly a combination of two individual decay components as both AgNP and Au-GSH get excited with the 387 nm laser pulse. Because of the overlapping excitations in the coupled system, it is not possible to resolve the influence of individual systems on the excited state interaction between the two, with 387 nm laser pulse excitation.

Biphotonic Excitation to Activate Plasmonic Ag Nanoparticles. One way to probe the excited state interaction between AgNP and Au-GSH is to use an excitation wavelength that is responded to by a single component of the coupled system. By employing 775 nm excitation, it is possible to induce a biphotonic excitation of AgNP. For example, AgNP deposited on Al_2O_3 films show the plasmon dampening following the excitation with 775 nm laser pulse.[29] It should be noted that the two-photon excitation of AgNP is seen only at higher laser powers of 775 nm. We subjected AgNP, Au-GSH and AgNP/AuGSH deposited on Al_2O_3 films to 775 nm laser pulse excitation (40 mW/cm^2) in our transient absorption spectrophotometer. The laser pulse energy of 40 mW/cm^2 is well above the 15 mW/cm^2 threshold required to induce two-photon excitation of AgNP.[29] The difference absorption spectra recorded 1 ps after laser pulse excitation of AgNP/Au-GSH, as well as each of AgNP and Au-GSH deposited on Al_2O_3 films are shown in Figure 4A. Direct excitation of Au-GSH with similar laser power of 775 nm pulses (blue trace labeled 'b' in Figure 4A) did not produce an observable transient absorption. On the other hand, AgNP alone (spectrum a) and AgNP/Au-GSH (spectrum c) exhibit spectral features with distinct absorption changes in the visible region.

$$\text{Au-GSH} + n\text{h}\nu_{775\text{nm}} \rightarrow \text{No observed effect} \quad (4)$$

$$\text{AgNP} + n\text{h}\nu_{775\text{nm}} \rightarrow \text{AgNP*} \quad (5)$$

$$\text{Au-GSH/AgNP} + n\text{h}\nu_{775\text{nm}} \rightarrow \text{Au-GSH/AgNP*} \quad (6)$$

The biphotonic excitation (n = 2 in reactions 4−6) employed in the above experiment was intended to excite only Ag nanoparticles. However, the transient absorption spectrum recorded with AgNP/Au-GSH (Figure 4A, spectrum c) shows a drastically different spectral profile than the one recorded with AgNP alone (Figure 4A, spectrum a). The appearance of a broad absorption at wavelengths greater than 550 nm, which matches the characteristics of Au-GSH*, confirms formation of the excited state of the metal cluster through plasmonic interactions. It is important to note that this broad absorption at wavelengths >550 nm is seen only in the Au-GSH/AgNP coupled system. Another interesting difference lies in the magnitude of the transient bleaching assigned to excited AgNP (dampening of the plasmon absorption band). While the position of the bleaching maximum is unaffected, the magnitude of bleaching is significantly enhanced, indicating strong optical enhancement effects between the two photoactive systems of AgNP/Au-GSH film.

Figure 4B shows the transient absorption-time profiles recorded at 650 nm for each of the three samples (AgNP/Au-GSH, AgNP alone, and AuGSH alone). The 650 nm excited state absorption signal for Au-GSH* is seen only when both AgNP and Au-GSH are present in the coupled system. Excitation of surface plasmons has been shown to enhance optical transitions of neighboring materials, this is commonly referred to as the plasmon enhancement mechanism.[7,30,31] This

DOI: 10.1021/acs.jpclett.5b00665
J. Phys. Chem. Lett. 2015, 6, 1870−1875

enhancement occurs for both linear as well as two-photon transitions of molecules in the vicinity of metal NPs.[32] The results presented here ascertain that the plasmon enhancement of AgNP induces excitation of Au-GSH when they are coupled.

Another point to note is the lifetime of excited Au-GSH in the coupled system. The Au-GSH excited state achieved through plasmon excitation has a significantly lower lifetime than the lifetime of ~780 μs, obtained through direct excitation at 387 nm (and the absence of nanoparticles).[22] The lifetime of the excited state as monitored from the transient decay at 650 nm has a lifetime of 1.01 ± 0.06 ps (Figure 4B). The decreased lifetime of Au-GSH* in the coupled system is an indication that the excited state is quenched by Ag nanoparticles. Similar quenching has also been observed in the Au-GSH/AuNP coupled system (see Figure S5). It is well-known that nanoparticles are very good quenchers of excited states, since they participate in energy and electron transfer processes.[30,33−35] The interaction between metal and excited semiconductor quantum dots has also been shown to decrease the lifetime of quantum dots. For example, CdSe quantum dots when coupled to a silver surface exhibit a rapid relaxation as the excited state lifetimes of CdSe decreases from 941 to 62 ps.[36] The quenching of Au-GSH* by Ag nanoparticles evidenced here should not be interpreted as energy transfer processes. If this was the case, we would have seen a growth in the plasmon excitation of Ag or Au nanoparticles over decay time scales of Au-GSH* clusters. We attribute the observed quenching effects to non-radiative deactivation of processes for Au-GSH in contact with AgNP. In addition, we also consider evidence for hot electron injection from excited Ag nanoparticles into gold clusters on these time scales to be negligible.

Power Dependence. The excited state interaction between Au-GSH and Ag nanoparticles is further exemplified by tracking the power dependence on both plasmon excitation (measured by the maximum plasmon bleach) and the yield of the Au-GSH* (as measured from the absorption magnitude at 650 nm). The results are compared in Figure 4C and D, respectively. As determined earlier,[29] two-photon excitation of nanoparticles has a threshold of ~15 mW/cm^2, below which there are no observable transient absorbance changes following 775 nm laser pulse excitation. With increasing laser power we see an increased plasmon bleach in both AgNP and Au-GSH/AgNP films (Figure 4C). The Au-GSH* yield, as measured from the magnitude of 650 nm absorbance, also shows a similar power dependent increase, thus confirming the interplay between the two components of the coupled system (Figure 4D). Blank experiments carried out with Au-GSH do not show any noticeable absorption even at very high laser excitation power. The transient absorption versus excitation power is fit to eq 7 for Figure 4C,D, where N is a normalizing constant and the exponent η is the order of the process.

$$\Delta A = N \times (\text{laser power})^{\eta} \quad (7)$$

In all cases, η is greater than 1, indicating a nonlinear (biphotonic) excitation leading to the observed transient signal.

Synergy between Au-GSH and AgNP. The monophotonic and biphotonic excitations employed in this study identify the role of individual components. Under visible excitation below 450 nm, the system is activated by single photon excitation. The increased optical response of both Au-GSH clusters and AgNP in our coupled nanostructures, with 775 nm excitation, confirms a synergistic effect between AgNP and Au-GSH when they are coupled together. As a result of this synergy, we see plasmon excitation that enhances the formation of the Au-GSH* excited state as well as quenching of Au-GSH* by AgNP. Scheme 1 illustrates the excited state interaction in the AgNP/Au-GSH coupled system leading to enhanced optical response.

Scheme 1. Synergistic Optical Enhancement Between Excited AgNP and AuGSH

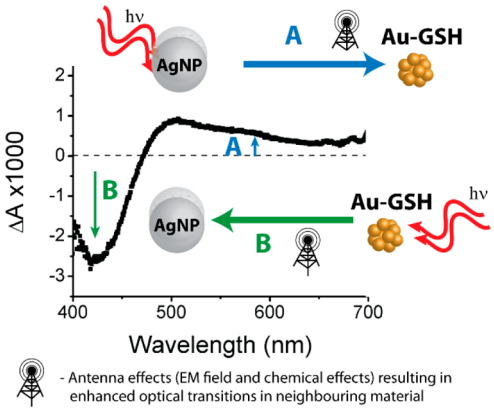

Plasmon enhancement of metal nanoparticles has made significant strides in optics, spectroscopy, and light harvesting applications. Plasmon excitation often results in enhanced optical activity via mechanisms, including enhancement of optical transitions, increased charge separation, and electronic interactions between metal/semiconductors.[37] The results presented here show that coupling with metal nanoclusters can further enhance the plamonic effect of metal nanoparticles.

Thiol protected gold clusters have recently been reported as photosensitizers in light harvesting for water splitting and photovoltaics.[27,38] Hence the effect of such small metal clusters should be taken into account when evaluating the performance of nanoparticles. In fact, when a metal nanoparticle is exposed to strong bonding ligands such as thiols, the surface can undergo transformation, and the metal clusters form a shell around the metal core. In fact, Ag nanoparticles having a shell of Ag clusters have been characterized in an earlier study.[39] It is unclear at this stage whether such metal clusters play a role in the reported claims of direct electron injection from excited metal nanoparticles to semiconductors.[40−42] Since surface plasmon interaction could also activate small metal cluster excitation and lead to electron transfer, it is critical to establish whether or not such metal clusters are present when studying nanoparticle/semiconductor interactions.

METHODS

AuGSH Clusters. Glutathione protected clusters were synthesized using a previously reported method.[28] Briefly, aqueous solutions of $HAuCl_4$ (2.2 mM) and L-glutathione (3 mM) were mixed and heated at 70 °C for 24 h with stirring. Upon mixing, the precursor solutions initially turned from yellow to clear, indicating the formation of a Au(I)-glutathione complex. Upon heating, solutions then changed from clear to yellow. The solution became emissive under ultraviolet (blacklight) illumination, indicating the formation of clusters. To remove excess L-glutathione, samples were precipitated and washed with 3:1 acetone:water and resuspended in water for further use. As discussed in an earlier work, these clusters are a mixture

DOI: 10.1021/acs.jpclett.5b00665
J. Phys. Chem. Lett. 2015, 6, 1870−1875

of sizes with 29−43 Au atoms capped with an approximately equal number of L-glutathione molecules.

Al_2O_3 Supported Au/Ag Nanoparticles. Alumina supported AgNP and AuNP were made by a recently reported dip method.[29] Similar to the SILAR method that has become common for making metal oxide supported quantum dots,[43,44] the metal precursors for AuNP and AgNP are adsorbed from aqueous metal salt solutions (10 mM $AgNO_3$ or $HAuCl_4$) and subsequently reduced by dipping the same metal oxide support into 10 mM aqueous $NaBH_4$ solution. Images of Al_2O_3 films containing gold and silver nanoparticles are shown in Figure S1.

Au-GSH Adsorption onto Al_2O_3. After growth of nanoparticles on Al_2O_3 films, dipping films in aqueous Au-GSH at pH 4 were used to adsorb Au-GSH (as illustrated in Scheme 2). Films containing AgNP/AuNP and Au-GSH were characterized using UV−vis absorption spectroscopy as well as transmission electron microscopy (TEM). TEM images of Al_2O_3 with deposited AgNP and Au-GSH are shown in Figure 1A−D, as well as absorption spectra for each of the films in Figure 1E.

Scheme 2. Sequential Deposition of AgNP and Au-GSH on Al_2O_3 Substrate

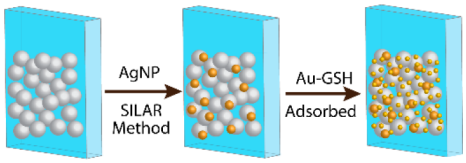

Femtosecond Transient Absorption Measurements. Ultrafast transient absorption techniques were performed using a Clark laser with a 775 nm fundamental pulsed at 1 kHz with 130 fs fwhm pulse durations. The fundamental is split to generate a white light probe by focusing through a Ti- Sapphire crystal. For 387 nm excitation, the second harmonic of the 775 nm is generated and used to excite samples. In this pump−probe setup, the transient absorption spectrum is recorded as a difference between probe signals obtained with and without a pump pulses. The delay between pump and probe is controlled through the optical delay rail to generate spectra at varied times following excitation. Transient absorption measurements were performed on films that were under vacuum, to ensure an inert atmosphere.

■ ASSOCIATED CONTENT

Supporting Information

Synthesis and UV−vis absorption spectra of Al_2O_3 films containing AuNP/Au-GSH and fsTAS data for AuNP/Au-GSH films excited with 387/775 nm laser pulses. Also, solution quenching of Au-GSH* with Ag and AuNP and Stern−Volmer analysis. The Supporting Information is available free of charge on the ACS Publications website at DOI: 10.1021/acs.jpclett.5b00665.

■ AUTHOR INFORMATION

Corresponding Author

*E-mail: pkamat@nd.edu; website: url:kamatlab.com.

Notes

The authors declare no competing financial interest.

■ ACKNOWLEDGMENTS

The research described herein was supported by the Division of Chemical Sciences, Geosciences and Biosciences, Basic Energy Sciences, Office of Science, U.S. Department of Energy through grant no. DE-FC02-04ER15533. This is document no. NDRL 5056 from Notre Dame Radiation Laboratory.

■ REFERENCES

(1) Eustis, S.; El-Sayed, M. Why Gold Nanoparticles are More Precious Than Pretty Gold: Noble Metal Surface Plasmon Resonance and Its Enhancement of the Radiative and Nonradiative Properties of Nanocrystals of Different Shapes. *Chem. Soc. Rev.* **2006**, *35*, 209−217.
(2) Quinten, M. The Color of Finely Dispersed Nanoparticles. *Appl. Phys. B: Lasers Opt.* **2001**, *73*, 317−326.
(3) Stamplecoskie, K. S.; Scaiano, J. C. Light Emitting Diode Irradiation Can Control the Morphology and Optical Properties of Silver Nanoparticles. *J. Am. Chem. Soc.* **2010**, *132*, 1825−1827.
(4) Coronado, E. A.; Encina, E. R.; Stefani, F. D. Optical Properties of Metallic Nanoparticles: Manipulating Light, Heat and Forces at the Nanoscale. *Nanoscale* **2011**, *3*, 4042−4059.
(5) Kelly, K. L.; Coronado, E.; Zhao, L. L.; Schatz, G. C. The Optical Properties of Metal Nanoparticles: The Influence of Size, Shape, and Dielectric Environment. *J. Phys. Chem. B* **2003**, *107*, 668−677.
(6) Stamplecoskie, K. G.; Grenier, M.; Scaiano, J. C. Self-Assembled Dipole Nanolasers. *J. Am. Chem. Soc.* **2014**, *136*, 2956−2959.
(7) Brus, L. Noble Metal Nanocrystals: Plasmon Electron Transfer Photochemistry and Single-Molecule Raman Spectroscopy. *Acc. Chem. Res.* **2008**, *41*, 1742−1749.
(8) Stamplecoskie, K. G.; Fasciani, C.; Scaiano, J. C. Dual-Stage Lithography from a Light-Driven, Plasmon-Assisted Process: A Hierarchical Approach to Subwavelength Features. *Langmuir* **2012**, *28*, 10957−61.
(9) Stamplecoskie, K. G.; Pacioni, N. L.; Larson, D.; Scaiano, J. C. Plasmon-Mediated Photopolymerization Maps Plasmon Fields for Silver Nanoparticles. *J. Am. Chem. Soc.* **2011**, *133*, 9160−3.
(10) Stamplecoskie, K. S.; Scaiano, J. C.; Tiwari, V. S.; Anis, H. Optimal Size of Silver Nanoparticles for Surface-Enhanced Raman Spectroscopy. *J. Phys. Chem. C* **2011**, *115*, 1403−1409.
(11) Aikens, C. M.; Li, S. Z.; Schatz, G. C. From Discrete Electronnic States to Plasmons: TDDFT Optical Absorption Properties of $Ag_{(n)}$ (n = 10, 20, 35, 56, 84, 120) Tetrahedral Clusters. *J. Phys. Chem. C* **2008**, *112*, 11272−11279.
(12) Guo, W.; Yuan, J.; Wang, E. Organic-Soluble Fluorescent Au_8 Clusters Generated from Heterophase Ligand-Exchange Induced Etching of Gold Nanoparticles and Their Electrochemiluminescence. *Chem. Commun.* **2012**, *48*, 3076−3078.
(13) Link, S.; El-Sayed, M.; Schaaff, T.; Whetten, R. Transition from Nanoparticle to Molecular Behaviour: A Femtosecond Transient Absorption Study of a Size Selected 28 Atom Gold Cluster. *Chem. Phys. Lett.* **2002**, *356*, 240−246.
(14) Qian, H.; Sfeir, M. Y.; Jin, R. Ultrafast Relaxation Dynamics of $[Au_{25}(SR)_{18}]^q$ Nanoclusters: Effects of Charge State. *J. Phys. Chem. C* **2010**, *114*, 19935−19940.
(15) Zhu, M.; Aikens, C. M.; Hollander, F. J.; Schatz, G. C.; Jin, R. Correlating the Crystal Structure of a Thiol-Protected Au_{25} Cluster and Optical Properties. *J. Am. Chem. Soc.* **2008**, *130*, 5883−5885.
(16) Negishi, Y.; Nakazaki, T.; Malola, S.; Takano, S.; Niihori, Y.; Kurashige, W.; Yamazoe, S.; Tsukuda, T.; Häkkinen, H. A Critical Size for Emergence of Nonbulk Electronic and Geometric Structures in Dodecanethiolate-Protected Au Clusters. *J. Am. Chem. Soc.* **2014**, *137*, 1206−1212.
(17) Jiang, D.; Overbury, S. H.; Dai, S. Structure of $Au_{15}(SR)_{13}$ and Its Implication for the Origin of the Nucleus in Thiolated Gold Nanoclusters. *J. Am. Chem. Soc.* **2013**, *135*, 8786−8789.
(18) Yu, Y.; Chen, X.; Yao, Q.; Yu, Y.; Yan, N.; Xie, J. Scalable and Precise Synthesis of Thiolated Au_{10-12}, Au_{15}, Au_{18}, and Au_{25} Nanoclusters via pH Controlled CO Reduction. *Chem. Mater.* **2013**, *25*, 946−952.

DOI: 10.1021/acs.jpclett.5b00665
J. Phys. Chem. Lett. 2015, 6, 1870−1875

(19) Tlahuice, A.; Garzón, I. On the Structure of the $Au_{18}(SR)_{14}$ Cluster. *Phys. Chem. Chem. Phys.* **2012**, *14*, 3737−3740.
(20) Yu, Y.; Luo, Z.; Chevrier, D. M.; Leong, D. T.; Zhang, P.; Jiang, D.; Xie, J. Identification of a Highly Luminescent $Au_{22}(SG)_{18}$ Nanocluster. *J. Am. Chem. Soc.* **2014**, *136*, 1246−1249.
(21) Qian, H.; Jiang, D.; Li, G.; Gayathri, C.; Das, A.; Gil, R. R.; Jin, R. Monoplatinum Doping of Gold Nanoclusters and Catalytic Application. *J. Am. Chem. Soc.* **2012**, *134*, 16159−16162.
(22) Stamplecoskie, K. G.; Chen, Y. S.; Kamat, P. V. Excited-State Behavior of Luminescent Glutathione-Protected Gold Clusters. *J. Phys. Chem. C* **2014**, *118*, 1370−1376.
(23) Stamplecoskie, K. G.; Kamat, P. V. Size-Dependent Excited State Behavior of Glutathione-Capped Gold Clusters and Their Light-Harvesting Capacity. *J. Am. Chem. Soc.* **2014**, *136*, 11093−11099.
(24) Choi, H.; Chen, W. T.; Kamat, P. V. Know Thy Nano Neighbor. Plasmonic versus Electron Charging Effects of Metal Nanoparticles in Dye-Sensitized Solar Cells. *ACS Nano* **2012**, *6*, 4418−4427.
(25) Hägglund, C.; Apell, S. P. Plasmonic Near-Field Absorbers for Ultrathin Solar Cells. *J. Phys. Chem. Lett.* **2012**, *3*, 1275−1285.
(26) Thomann, I.; Pinaud, B. A.; Chen, Z.; Clemens, B. M.; Jaramillo, T. F.; Brongersma, M. L. Plasmon Enhanced Solar-to-Fuel Energy Conversion. *Nano Lett.* **2011**, *11*, 3440−3446.
(27) Chen, Y. S.; Choi, H.; Kamat, P. V. Metal-Cluster-Sensitized Solar Cells. A New Class of Thiolated Gold Sensitizers Delivering Efficiency Greater than 2%. *J. Am. Chem. Soc.* **2013**, *135*, 8822−8825.
(28) Luo, Z.; Yuan, X.; Yu, Y.; Zhang, Q.; Leong, D. T.; Lee, J. Y.; Xie, J. From Aggregation-Induced Emission of Au(I)-Thiolate Complexes to Ultrabright Au(0)@Au(I)-Thiolate Core−Shell Nanoclusters. *J. Am. Chem. Soc.* **2012**, *134*, 16662−16670.
(29) Stamplecoskie, K. G.; Manser, J. S. Facile SILAR Approach to Air-Stable Naked Silver and Gold Nanoparticles Supported by Alumina. *ACS Appl. Mater. Interfaces* **2014**, *6*, 17489−17495.
(30) Pacioni, N. L.; González-Béjar, M. G.; Alarcon, E.; McGilvray, K.; Scaiano, J. C. Surface Plasmons Control the Dynamics of Excited Triplet States in the Presence of Gold Nanoparticles. *J. Am. Chem. Soc.* **2010**, *132*, 6298−6299.
(31) Scaiano, J. C.; Netto-Ferreira, J. C.; Alarcon, E.; Billone, P.; Alejo, C. J. B.; Crites, C. O.; Decan, M.; Fasciani, C.; González-Béjar, M. G.; Hallett-Tapley, G.; Grenier, M.; Mcgilvray, K.; Pacioni, N. L.; Pardoe, A.; René-Boisneuf, L.; Schwartz-Narbonne, R.; Silvero, J.; Stamplecoskie, K. G.; Wee, E. Tuning Plasmon Transitions and Their Applications in Organic Photochemistry. *Pure Appl. Chem.* **2011**, *83*, 913−930.
(32) Sivapalan, S. T.; Vella, J. H.; Yang, T. K.; Dalton, M. J.; Swiger, R. N.; Haley, J. E.; Cooper, T. M.; Urbas, A. M.; Tan, L.; Murphy, C. J. Plasmonic Enhancement of the Two Photon Absorption Cross Section of an Organic Chromophore Using Polyelectrolyte-Coated Gold Nanorods. *Langmuir* **2012**, *28*, 9147−9154.
(33) Yang, T.-T.; Chen, W.-T.; Hsu, Y.-J.; Wei, K.-H.; Lin, T.-Y.; Lin, T.-W. Interfacial Charge Carrier Dynamics in Core−Shell Au−CdS Nanocrystals. *J. Phys. Chem. C* **2010**, *114*, 11414−11420.
(34) Pramod, P.; Sudeep, P. K.; Thomas, K. G.; Kamat, P. V. Photochemistry of Ruthenium Trisbipyridine Functionalized on Gold Nanoparticles. *J. Phys. Chem. B* **2006**, *110*, 20737−20741.
(35) Thomas, K. G.; Kamat, P. V. Chromophore-Functionalized Gold Nanoparticles. *Acc. Chem. Res.* **2003**, *36*, 888−898.
(36) Gómez, D. E.; Lo, S. S.; Davis, T. J.; Hartland, G. V. Picosecond Kinetics of Strongly Coupled Excitons and Surface Plasmon Polaritons. *J. Phys. Chem. B* **2013**, *117*, 4340−4346.
(37) Kale, M. J.; Avanesian, T.; Christopher, P. Direct Photocatalysis by Plasmonic Nanostructures. *ACS Catal.* **2014**, *4*, 116−128.
(38) Chen, Y. S.; Kamat, P. Glutathione Capped Gold Nanoclusters as Photosensitizers. Visible Light Induced Hydrogen Generation in Neutral Water. *J. Am. Chem. Soc.* **2014**, 140326112920004.
(39) Diez, I.; Ras, R. H. A. Fluorescent Silver Nanoclusters. *Nanoscale* **2011**, *3*, 1963−1970.
(40) Hoggard, A.; Wang, L.; Ma, L.; Fang, Y.; You, G.; Olson, J.; Liu, Z.; Chang, W.; Ajayan, P. M.; Link, S. Using the Plasmon Linewidth To Calculate the Time and Efficiency of Electron Transfer between Gold Nanorods and Graphene. *ACS Nano* **2013**, *7*, 11209−11217.
(41) Reineck, P.; Lee, G.; Brick, D.; Karg, M.; Mulvaney, P.; Bach, U. A Solid-State Plasmonic Solar Cell via Metal Nanoparticle Self-Assembly. *Adv. Mater.* **2012**, *24*, 4750−4755.
(42) Long, R.; Prezhdo, O. V. Instantaneous Generation of Charge-Separated State on TiO_2 Surface Sensitized with Plasmonic Nanoparticles. *J. Am. Chem. Soc.* **2014**, *136*, 4343−4354.
(43) Nicolau, Y. F. Solution Deposition of Thin Solid Compound Films by a Successive Ionic-Layer Adsorption and Reaction Process. *Appl. Surf. Sci.* **1985**, *22*−*23* (Part 2), 1061−1074.
(44) Kale, R. B.; Sartale, S. D.; Chougule, B. K.; Lokhande, C. D. Growth and Characterization of Nanocrystalline CdSe Thin Films Deposited by the Successive Ionic Layer Adsorption and Reaction Method. *Semicond. Sci. Technol.* **2004**, *19*, 980−986.

DOI: 10.1021/acs.jpclett.5b00665
J. Phys. Chem. Lett. 2015, 6, 1870−1875